View metadata, citation and similar papers at core.ac.uk

brought to you by CORE

provided by Elsevier - Publisher Connector

ELSEVIER

Biochimica et Biophysica Acta 1421 (1999) 53–63

BIOCHIMICA ET BIOPHYSICA ACTA

BBA

www.elsevier.com/locate/bba

Correlation between anti-bacterial activity and pore sizes of two classes of voltage-dependent channel-forming peptides

Laure Béven [a], Olivier Helluin [b,1], Gérard Molle [b], Hervé Duclohier [b], Henri Wróblewski [a,*]

[a] *Université de Rennes 1, UPRES-A CNRS 6026, GDR CNRS 790, Campus de Beaulieu, 35042 Rennes Cedex, France*

[b] *Université de Rouen, UMR CNRS 6522, GDR CNRS 790, IFRMP 23, Boulevard Maurice de Broglie, 76821 Mont-Saint-Aignan Cedex, France*

Received 8 April 1999; received in revised form 21 June 1999; accepted 28 June 1999

Abstract

Anti-bacterial activities were compared for two series of voltage-dependent pore-formers: (i) alamethicin (Alm) and its synthetic analogs (Alm-dUL) where α-amino-isobutyric acid residues (Aibs) were replaced by leucines and selected key residues substituted and (ii) homologous voltage sensors of the electric eel sodium channel (repeats S4L45 (III) and S4L45 (IV)). *Spiroplasma melliferum*, a bacterium related to the mycoplasmas, was used as a target cell. The data show that with respect to growth inhibition, cell deformation and plasma membrane depolarization, the highest efficient peptide remained natural Alm although the minimal inhibitory concentrations of its Leu analogs were within the same range as the parent molecule, except for Alm-dUL P14A. Thus, as for the pore-forming activity observed in artificial membranes and for the toxicity towards mammalian cells, proline-14 proved to be a critical residue for the anti-bacterial activity of alamethicin. Regarding the sodium voltage sensors, their anti-bacterial efficiency was at least 10 times lower although they promoted spiroplasma cell agglutination. The anti-bacterial activities of the peptides were correlated with their pore-forming properties, especially with the apparent and mean number of monomers per conducting aggregate ($\langle N \rangle$) when both peptide families were considered and, secondly, with mean open times (τ_o) within each family. This suggests that although they may form 'raft-like' structures, the mechanism underlying anti-bacterial activity of Alm and its active analogs, as well as the S4L45 voltage sensors with the *S. melliferum* plasma membrane, is predominantly through pore-formation according to the 'barrel-stave' mechanism. © 1999 Elsevier Science B.V. All rights reserved.

Keywords: Alamethicin; Anti-bacterial activity; Pore-former; Voltage sensor; *Spiroplasma melliferum*

Abbreviations: AC, agglutinating concentration; Alm, alamethicin; CFU, colony-forming unit; DAPI, 4′,6-diamidino-2-phenylindole; DC, deforming concentration; $diSC_3$-(5), 3,3′-dipropyl-2,2′-thiadicarbocyanine iodide; DOPE, 1,2-dioleoyl phosphatidylethanolamine; HEPES, (hydroxy-2-ethyl-4-piperazinyl-1)-2-ethane sulfonic acid; MIC, minimal inhibitory concentration; MLC, minimal lethal concentration; $\langle N \rangle$, apparent and mean number of monomers per conducting aggregate; POPC, 1-palmitoyl, 2-oleoyl phosphatidylcholine; $\Delta\psi$, transmembrane electrical potential; τ_o, channel mean open time

* Corresponding author. Tel.: 33-2-99-28-61-38; Fax: 33-2-99-28-67-00; E-mail: wroblews@univ-rennes1.fr

[1] Present address: Department of Biochemistry and Biophysics, University of Pennsylvania School of Medicine, Philadelphia, PA 19104, USA.

0005-2736/99/$ – see front matter © 1999 Elsevier Science B.V. All rights reserved.
PII: S0005-2736(99)00111-X

1. Introduction

Amphipathic peptides endowed with antibiotic activity play a major role in the competition opposing living organisms for the occupancy of ecological niches (for review, see [1,2]). Indeed, such peptides are used by complex organisms as defence molecules against microbial infections as well as produced by eukaryotic and prokaryotic microorganisms [1,3]. Although these molecules display as a whole considerable sequence diversity, they are short (usually less than 40 residues), amphipathic and often cationic [4–6]. Partly reflecting this diversity, there is no general agreement for the molecular mechanisms underlying their anti-microbial activity apart from assuming the induction of structural-functional perturbations in the membranes of target cells [7]. In particular, attempting to correlate the anti-bacterial activity with the pore-forming ability that many of these peptides display in model membranes remains, to some extent, a matter of debate. For example, charged amphipathic peptide helices, especially melittin, have been demonstrated to induce non-bilayer phases at a range of intermediate to high peptide concentrations [8], whilst magainins, sometimes qualified as 'peptidergents', form large water-filled membrane disruptions rather than the pores observed in conductance experiments. If discrete ion channels may be occasionally observed at low magainin concentrations [9], it is now assumed that these pores, which formation is much favored at higher concentrations, would be toroidal, lined by negatively charged lipids strongly bound to cationic magainin helices that would not self-aggregate [10].

Contrasting with the abundant literature dealing with anti-bacterial activities of cationic peptides, e.g. magainins, cecropins and defensins (which incidentally are poor channel-formers [11]), the corresponding data are scanty for alamethicin (Alm) apart from an initial study [12]. Alamethicin is a linear 20 residue peptaibol produced by the soil fungus *Trichoderma viride* [13] and contains eight residues of the helix-promoting α-amino-isobutyric acid (Aib). Its antibiotic activity is illustrated by its toxicity towards mollicutes (wall-less eubacteria) [14,15], Gram-positive eubacteria [12] and diverse mammalian cell lines [16]. Furthermore, Alm is still certainly the best characterized channel-forming peptide having indeed been subjected to many biophysical studies over the last two decades (for review, see [17,18]). There is now a consensus for the 'barrel-stave' model in which intramembrane aggregates are made by the juxtaposition of Alm monomers, their amphiphilic sectors defining the conducting pores [19]. The apparent average number of monomers ($\langle N \rangle$) building up the pores can most easily be derived from the analysis of macroscopic current-voltage curves which also show the essential property of high voltage-dependence (see below and [20]). There is also an agreement between $\langle N \rangle$ and the most probable substate at the single-channel level which shows fluctuations between substates reflecting the uptake and release of monomers into the conducting bundle.

The relevance of these conductance studies in attempting to explain anti-bacterial activity is far from being straightforward as not only targets are different as well as the sensitivities of the respective assays, but concentrations may often differ by 1–3 orders of magnitude. This difficulty may be partly overcome by the comparison of mutants or synthetic variants of the same molecule and/or distinct classes of molecules displaying similar activities. Indeed, in the case of Alm, if we assume for now that the anti-bacterial activity reflects pore formation, then, selected substitutions of key residues affecting the conductance parameters and in particular the size of the pores should equally have consequences on the efficacy of the analogs in the anti-bacterial assays. We thus took the opportunity of a complete set of conductance data recently obtained on a series of Alm synthetic analogs where some substitutions affected the apparent number of monomers involved in the pores (according to the 'barrel-stave' model) to search if any positive correlations could be drawn with anti-bacterial activity. As a control, we also assayed two other peptides, unrelated to the Alm family although showing a similar voltage-dependence and also functioning through monomer aggregation, but with a significantly reduced pore size. Reproducing the homologous voltage sensors (S4s) of domains III and IV of the sodium channel extended with the L45 linkers (binding sites for the 'inactivating particle' [21]), these peptides present arginines every three residues along their sequences. As a target cell, we used *Spiroplasma melliferum*, a helically shaped bacterium belonging to the mollicutes

[22]. This choice was dictated by two main reasons. Firstly, the plasma membrane of *S. melliferum* is directly accessible to exogenous peptides owing to the absence of a cell wall and of an outer membrane [23,24]. Secondly, motility inhibition and cell deformation are very sensitive indicators of spiroplasma membrane perturbation [14,15,25,26]. The data obtained in this study clearly show that indeed a correlation can be drawn between anti-bacterial efficacy and the size of pores.

2. Materials and methods

2.1. S. melliferum strain and culture conditions

The strain BC-3^T (ATCC 33219) of *S. melliferum* [22] was grown under micro-aerobic conditions at 32°C in BSR medium containing 5% horse serum and 2 mM (hydroxy-2-ethyl-4-piperazinyl-1)-2-ethane sulfonic acid (HEPES) [27].

2.2. Peptides preparation and characterization

Alm F50 from *T. viride* was obtained from Sigma (St. Louis, MO, USA). Synthesis, purification, mass and secondary structure determinations of the other peptides used in this study (Fig. 1) are extensively described elsewhere [28–31].

2.3. Anti-bacterial assays

The minimal inhibitory concentration (MIC) of each peptide was determined by the broth dilution method. Serial 2-fold dilutions of the peptides were made in BSR medium containing 5% horse serum and 2 mM HEPES (see above) in 96-well microtiter plates as described previously [14]. The starting spiroplasma concentration in each well was 10^6 colony-forming units (CFU) per ml. The MICs were determined after a 48-h incubation of the plates at 32°C and taken as the lowest peptide concentrations at which growth was fully inhibited. To distinguish bacteriostatic effects from bactericidal ones, spiroplasma cells (10^6 CFU/ml) were incubated for 2 h in liquid BSR medium containing peptides or not and plated on solid BSR medium devoid of peptide. The plates were subsequently incubated at 32°C and examined daily for the formation of colonies. The minimal lethal concentration (MLC) was defined as the lowest peptide concentration killing at least 99% of the cells. All assays were performed in triplicate.

2.4. Light microscopy

All the experiments were performed on spiroplasma cell suspensions containing 10^{10} CFU/ml ($A_{600} = 1.0$) in 50 mM sodium phosphate buffer (pH 7.0), 50 mM D-glucose and 549 mM D-sorbitol. Dark-field optics were used as described previously [14,15,25] to analyze the effects of the peptides on spiroplasma motility and cell morphology. The 4′,6-diamidino-2-phenylindole (DAPI) technique [32] was used to assess the presence of DNA within the spiroplasma cells. In this case, the cells were treated with different peptide concentrations and subsequently fixed for 2 h with 2.5% glutaraldehyde at room temperature. After washing with deionized water, the cells were stained for 15 min with 10 μg DAPI/ml, washed again in water and observed by reflected light fluorescence using the Leica Diaplan microscope, the Leica filter cube D, the 3λ-Ploemopak illuminator and the Leitz PL Fluotar oil immersion objective ($\times 100$, $NA = 1.32$). Micrographs were taken with the Nikon F-801 camera using Ilford HP 5 Plus 35 mm film (ISO 400).

2.5. Measurement of the membrane potential

Exponentially growing spiroplasma cells were harvested, washed once in 5 mM HEPES buffer, pH 7.0, containing 128 mM NaCl and 50 mM D-glucose. Finally, the cells were dispersed into the same buffer to obtain a density of 10^9 CFU/ml ($A_{600} = 0.10$, 30 μg of cell protein/ml) and the membrane potential was measured using the fluorescent potentiometric dye 3,3′-dipropyl-2,2′-thiadicarbocyanine iodide as described previously [15,25].

2.6. Pore-forming activity in planar lipid bilayers

Anti-bacterial activities of the peptides were compared with conductance parameters in planar lipid bilayers under the applied voltage, issued from previously published studies [29–31,33]. Since the methodology is quite different from the above-described

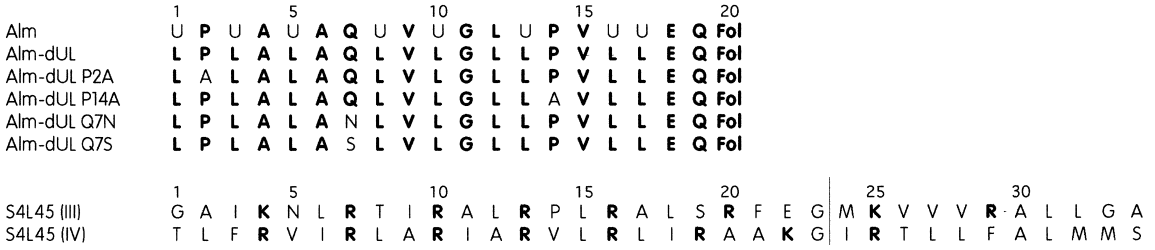

Fig. 1. Amino acid sequences of the peptides assayed. Except phenylalaninol (Fol), the amino acid residues are designated by their one-letter code, with U standing for Aib. In the Alm series, residues shared with Alm-dUL are in bold. In the S4L45 peptides, positively charged residues (K, lysine and R, arginine) are in bold. The vertical bar indicates the border between S4 and L45 amino acid stretches.

anti-bacterial assays, it is useful in the context of the present study to briefly summarize the bilayer methods then used as well as the significance of the selected conductance parameters. In macroscopic conductance experiments, virtually solvent-free neutral lipid bilayers made from 1-palmitoyl, 2-oleoyl phosphatidylcholine (POPC)/1,2-dioleoyl phosphatidylethanolamine (DOPE) (7/3 by mass) phospholipid monolayers were formed over a 200-μm hole in a thin teflon film separating the *cis* and *trans* chambers containing the electrolyte. Peptides were added to the *cis* or positive compartment in the concentration range 10^{-8}–10^{-7} M in the case of Alm analogs and 10^{-7}–10^{-6} M for the voltage sensors. After equilibration with the bilayers, the latter were submitted to slow voltage ramps. Both classes of peptides then induced a highly voltage-dependent current, V_e being the voltage increment inducing an *e*-fold change in conductance (see Fig. 6). Furthermore, the threshold for the development of the current exponential branch is dependent on the peptide concentration, V_a being the voltage shift of the threshold resulting from an *e*-fold change in concentration. As demonstrated earlier [20], the apparent and mean number of monomers in the barrel-stave forming the pore is then simply estimated as $\langle N \rangle = V_a / V_e$.

3. Results

3.1. Effect of the peptides on the growth of spiroplasma cells

In the Alm series, the six peptides inhibited the

Table 1
Comparison of the effects of the peptides on *S. melliferum* BC-3^T with published conductance data

Peptides	Anti-bacterial activities				Conductance data		
	MIC (μM)	MLC (μM)	DC_{50} (μM)	AC_{50} (μM)	V_e (mV)	$\langle N \rangle$	τ_o (ms)
Alm	6.25	12.5	0.25	–	6	10	50
Alm-dUL	12.5	25	0.5	–	7	8	2
Alm-dUL P2A	25	50	1	–	8	9	1.2
Alm-dUL P14A	100	–	4	–	7	6	0.3
Alm-dUL Q7N	12.5	25	0.5	–	9	9	2
Alm-dUL Q7S	50	100	2	–	7	7	1
S4L45 (III)	100	–	1	6.25	6	4	20
S4L45 (IV)	50	–	1	6.25	19	4–5	160

MIC, minimal peptide concentration necessary for a full inhibition of spiroplasma cell growth; MLC, minimal lethal concentration, i.e. the minimal peptide concentration capable of killing ≥99% spiroplasma cells after 2 h in liquid culture medium (Alm-dUL P14A and the two S4L45 peptides proved to be bacteriostatic (–) in the concentration range in which they were used); DC_{50}, concentration deforming 50% of the cells; AC_{50}, concentration agglutinating 50% of the cells. Alm and its synthetic Leu analogs (Alm-dUL) failed to agglutinate the cells (–). V_e and $\langle N \rangle$, macroscopic conductance parameters in planar lipid bilayers: the voltage increment producing an *e*-fold conductance change and the apparent mean number of peptide monomers per conducting aggregate, respectively. τ_o, mean open time of the most probable single-channel substate. These conductance parameters are issued from previous studies [28,30,31,33].

growth of *S. melliferum* with MICs ranging from 6.25 to 100 μM (Table 1). All of them except Alm-dUL P14A (see below) proved to be bactericidal in the concentration range used for the assays (i.e. up to 100 μM) and the MLCs proved to be equal to twice the corresponding MICs. The substitution of all the Aib residues (U) of Alm by Leu residues (Alm-dUL) made the peptide only twice less effective than the natural product. The activity of Alm-dUL was not modified by the additional conservative substitution Gln-7-Asn (Alm-dUL Q7N). In contrast, nonconservative substitutions further decreased the activity of the peptide, the strongest effect being observed in the case of Alm-dUL P14A (MIC = 100 μM) in which Pro-14 was replaced by Ala. In comparison, the voltage sensors of the electric eel sodium channel were

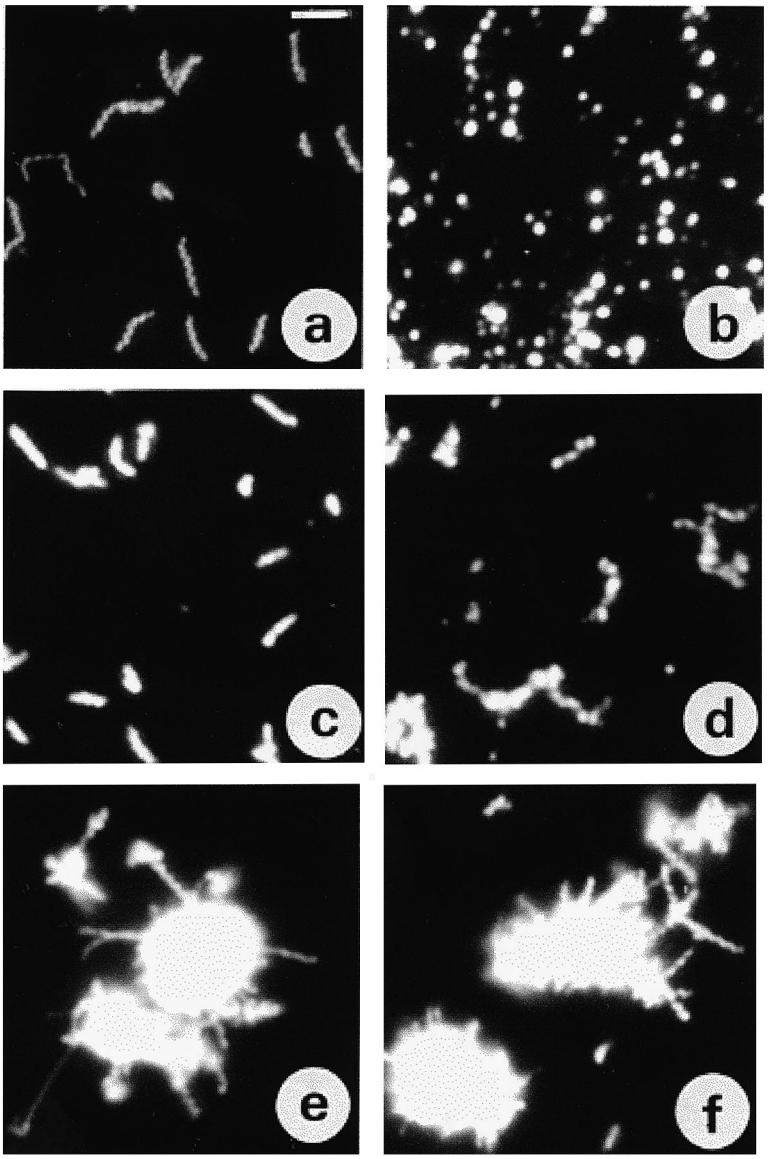

Fig. 2. Dark-field light microscopy observation of the effects of the peptides on spiroplasma cells. Untreated *S. melliferum* BC-3^T cells (a) are compared with cells treated for 10 min with 5 μM Alm (b), 5 μM Alm-dUL P14A (c), 5 μM Alm-dUL (d), 10 μM S4L45 (IV) (e) or 10 μM S4L45 (III) (f). Cell concentration, 10^{10} CFU/ml of 50 mM sodium phosphate buffer (pH 7.0) containing 50 mM D-glucose and 549 mM D-sorbitol. Bar (top right corner in a), 4 μm.

much less potent: S4L45 (III) and S4L45 (IV) exhibited MICs of 100 and 50 μM, respectively. Furthermore, no bactericidal effect could be observed for these two peptides in the 0–100 μM concentration range.

3.2. Spiroplasma cell deformation and agglutination

Exponentially growing *S. melliferum* cells were helical and highly motile, exhibiting an average length of 6.5 ± 1.5 μm, with a pitch of about 1 turn/μm (Fig. 2a). Upon treatment with 5 μM Alm, an instant loss of motility was observed, followed by a series of successive deformations (helix stretching, formation of aneurisms, swelling of the aneurisms) with each cell being finally split into several rounded forms after about 10 min (Fig. 2b). In the same conditions, Alm-dUL deformed the cells up to the penultimate step (aneurism swelling, Fig. 2d) whereas Alm-dUL P14A induced only the first deformation step (Fig. 2c). The effects of S4L45 (III) and S4L45 (IV) were similar to those observed with Alm-dUL P14A but these peptides furthermore agglutinated the cells. The aggregates were very large, including often several 10s of cells (Fig. 2e and f).

The minimal concentrations deforming or agglutinating 50% of the cells (DC_{50} and AC_{50}, respectively) in a suspension containing 10^{10} CFU/ml are displayed in Table 1. The comparison of the data shows that the minimal cell deforming activities of the peptides were lower than their corresponding MICs but the relative efficiencies were essentially similar. Controls revealed that the differences between growth inhibition and cell deformation tests were in fact due to the presence of serum in the culture medium used for the determination of the MICs and the MLCs. Indeed, we observed that the addition of 5% horse serum (the concentration used in the culture medium) decreases about 10-fold the deforming activity of the peptides. This suggests that the intrinsic anti-bacterial activity of these peptides (i.e. without serum) is in fact one order of magnitude higher than suggested by growth inhibition assays.

DAPI staining and observation of *S. melliferum* cells by reflected light fluorescence microscopy revealed that DNA was distributed over the whole length of the helices in untreated cells and in cells treated with 10 μM S4L45 (Fig. 3a and b). In the case of cells treated with 5 μM Alm, intensely fluorescent vesicles were observed after 10 min (Fig. 3c) and smaller, non-fluorescent vesicles after 2 h (Fig. 3d). This indicates that the Alm-induced cytolysis with DNA release into the medium did not occur during the initial cascade of cell deformations but much later.

3.3. Effect of the peptides on the membrane potential of spiroplasma cells

In 5 mM HEPES buffer, pH 7.0, containing 128 mM NaCl and 50 mM D-glucose as the energy source, *S. melliferum* maintained a constant membrane potential of -68 ± 5 mV (dotted line in Fig. 4) for at least 30 min at room temperature. Addition of 2.5 μM Alm lead to a complete depolarization of the plasma membrane within 2 min. The same concentrations of S4L45 (III) and S4L45 (IV) also depolarized the membrane, but to a lesser extent and with slower rates, with S4L45 (IV) being slightly more

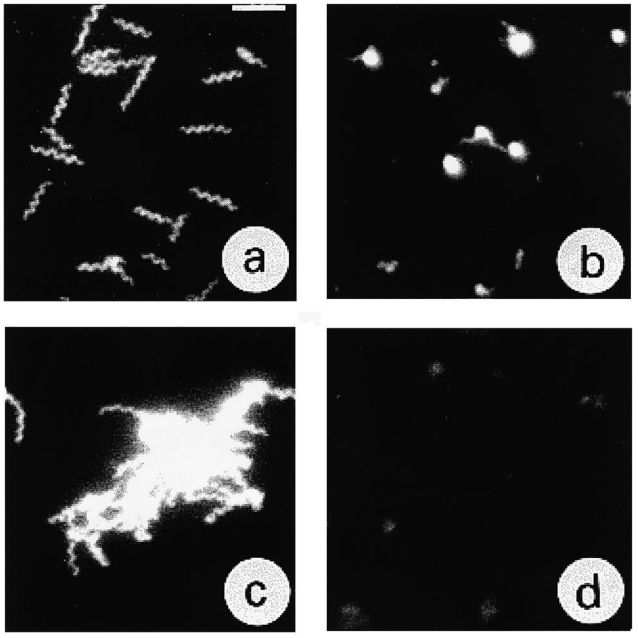

Fig. 3. Observation of peptide effects on spiroplasma cells by reflected light fluorescence microscopy. Untreated *S. melliferum* BC-3^T cells (a) are compared with cells treated with 5 μM Alm for 10 min (b), 10 μM S4L45 for 10 min (IV) (c) and 5 μM Alm for 2 h (d). The conditions were otherwise as in Fig. 2. DNA was stained with the fluorescent dye DAPI as described in the text. Bar (top right corner in a), 4 μm.

efficient than S4L45 (III). The dose-dependence curves confirmed the lower efficiency of S4L45 (IV) compared with Alm (Fig. 5). In the case of Alm, the membrane potential decreased almost linearly with the peptide concentration and a complete depolarization of the cell membrane was observed at a peptide concentration of 2 μM. In contrast, the curve of S4L45 (IV) proved to be biphasic in the same conditions: this peptide was as efficient as Alm for concentrations up to 1 μM but much less above this threshold since it failed to abolish the membrane potential even at a 10 μM concentration. It is a curious coincidence that this threshold (−40–−35 mV) approximately matches the one required for firing action potentials in excitable cells.

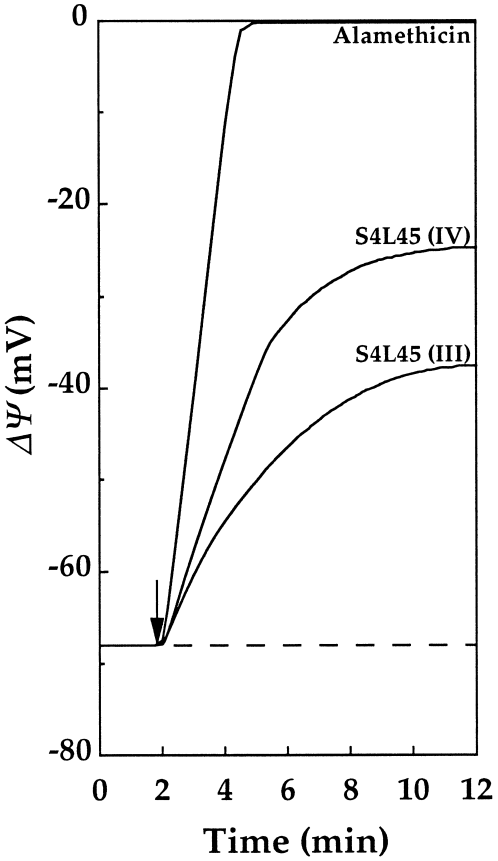

Fig. 4. Effect of the peptides on the membrane potential of *S. melliferum* BC-3^T cells. Spiroplasma cells (10^9 CFU/ml of 5 mM HEPES buffer, pH 7.0, 128 mM NaCl) were energized with 50 mM D-glucose. The dotted line corresponds to the membrane potential in the absence of peptide ($\Delta\Psi = 67 \pm 5$ mV, inside negative). The arrow indicates the time at which the peptides (final concentration, 2.5 μM) were added to the cell suspensions.

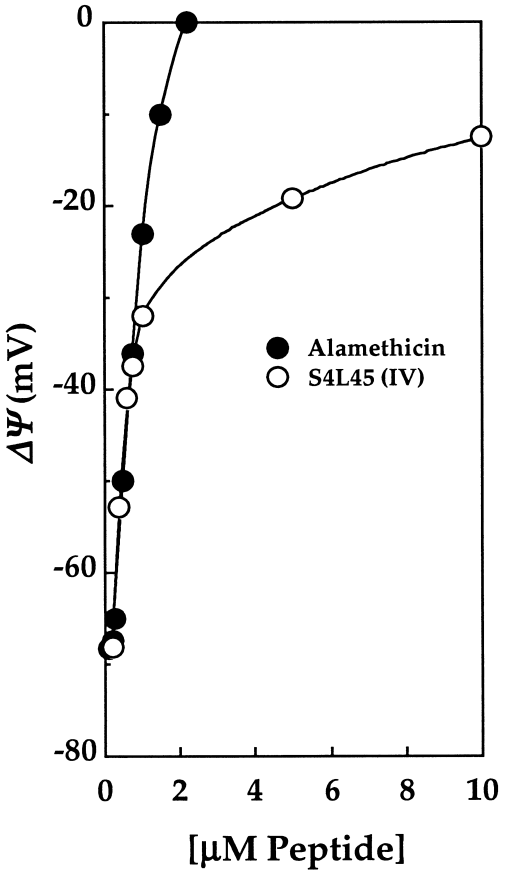

Fig. 5. Effect of Alm and S4L45 (IV) concentrations on the membrane potential ($\Delta\psi$) of *S. melliferum* BC-3^T cells. The same conditions as in Fig. 4.

4. Discussion

The two families of pore-forming peptides examined here for their anti-bacterial effects belong to two quite different classes with respect to origins, amino acid sequences and intrinsic functions. However, when interacting with large planar lipid bilayers under an applied electric field, macroscopic conductance experiments (where the number of expressed channels is in the order of 10^3) showed that these peptides have the common property of inducing high voltage-dependent currents. Indeed, V_e, the voltage increment that produces an *e*-fold in conductance, remained in the 5–10 mV range (Fig. 6) except for S4L45 (IV) (20 mV). As recalled above (Section 2), this allows for V_a, the concentration-dependence, a derivation of $\langle N \rangle$, i.e. the average number of monomers forming the pores.

In Fig. 7, the MICs are plotted as a function of

⟨*N*⟩. Overall, there is quite a good correlation between the two sets of data. Indeed, MICs steadily increase and thus, the peptides are less efficient in anti-bacterial activity assays as the pores become smaller. By contrast, no such correlation could be demonstrated with V_e alone. For instance, the polycationic S4L45s form the smallest conducting aggregates and are the poorest inhibitors despite a voltage-dependence that is quite similar to the Alm one. As expected, the positively charged voltage sensors do not fall on the same regression line drawn through the data for the Alm derivatives. However, despite being positively charged and apparently more akin to magainins and cecropins, their low anti-bacterial activity (similar to that of Alm-dUL P14A and Alm-dUL Q7N whose ⟨*N*⟩ values are 6 and 7, respectively) is associated with the lowest ⟨*N*⟩ (i.e. 4–5). In any case, our results are quite consistent with the limited anti-bacterial activities previously observed with the polycationic peptides $(XRL)_n$, with X being Ala, Val or Leu, designed as model voltage sensors [34]. The promotion of spiroplasma cell agglutination by S4L45 peptides reflects their high content of positive charges likely favoring intercellular ionic bridges. Interestingly, the same behavior (i.e. cell agglutination and poor anti-bacterial activity) has previously been reported for synthetic peptides containing a hydrophobic sequence and a polycationic C-terminal nuclear localization sequence [25]. A second correlation, albeit looser, can also be drawn upon inspection of Table 1 with the open times (τ_o) derived from single-channel analysis. Even within de S4L45 family, the homologue from domain IV displays single-channel events of longer duration and is slightly more efficient than homologue III. Thus, the larger and the more stable the channels, the more efficient are the peptides in anti-bacterial assays.

With respect to the first family, the parent natural peptaibol Alm remains the most active although the replacement of all its eight Aibs by Leu residues (in Alm-dUL) only halves the efficiency both in terms of spiroplasma growth inhibition and deformation (Table 1). Note that this is associated with a reduced pore size and faster kinetics at the single-channel level although V_e remained unaffected [30]. The correlation still applies with the next Alm derivatives

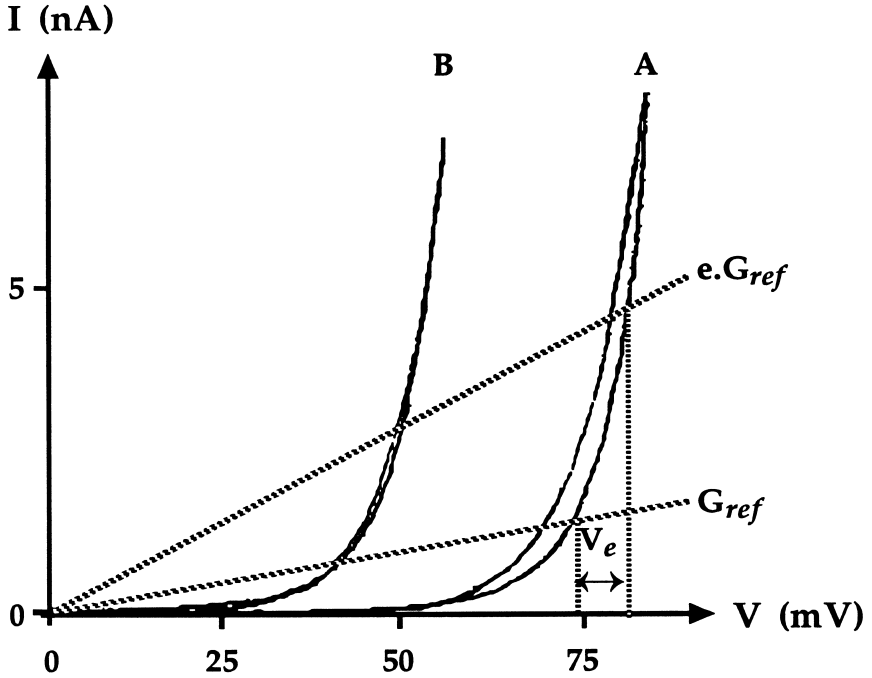

Fig. 6. Macroscopic current-voltage (I–V) curves for Alm-dUL at two concentrations: 5×10^{-8} M (curve A) and 10^{-7} M (curve B). In each case, three sweeps were superimposed. Electrolyte solution: 1 M KCl buffered to pH 7.4, both sides of a POPC:DOPE (7/3 by mass) bilayer. Room temperature. The voltage thresholds for the responses to attain an arbitrary reference conductance (G_{ref}) are pointed out for the two concentrations together with V_e, the voltage-dependence parameter.

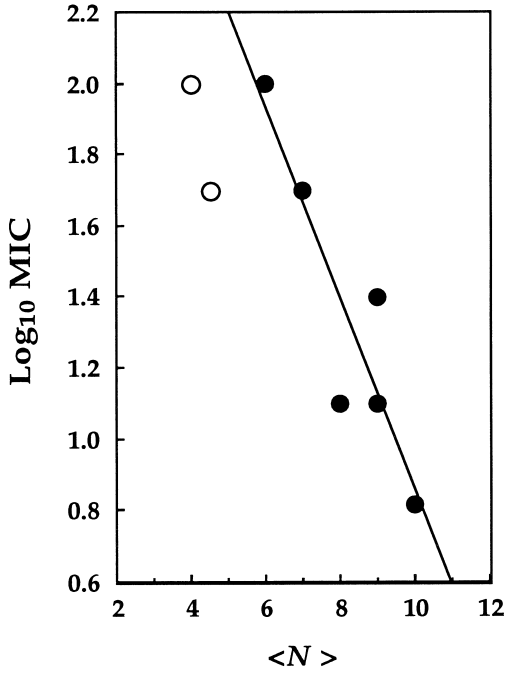

Fig. 7. Correlation with conductance parameters in planar lipid bilayers. The graph is a semi-log plot of MICs as a function of $\langle N \rangle$, the mean number of monomers per conducting aggregate estimated by the ratio of V_a and V_e (concentration and voltage-dependence parameters, respectively) derived from the macroscopic conductance (see Fig. 6 and Section 2). The regression line is drawn through the data for Alm derivatives (filled circles). The empty circles are for the S4L45 voltage sensors.

which were originally designed to test, by amino acid substitutions, the role of 'key positions' especially at Gln-7 [31] and Pro-14 [33] in the formation of pores according to the barrel-stave scheme. As a whole, effects of such substitutions on conductance parameters are matched here by modulation of the anti-bacterial activities in the expected direction. First, the conservative Q7N substitution does not affect the efficacy of Alm-dUL since the interhelical H-bonds are maintained as demonstrated in conductance experiments [31] and molecular modelling/dynamics [35]. As for the Q7S analog, although it allows conducting bundles, it does so with enhanced kinetics due to the destabilization of H-bonds [31] and this is matched by a MIC in the mid-range. On the other hand, the P14A substitution likely to affect helix bend, although maintaining a high voltage-dependence [33], has a drastic effect which also reflects the higher concentrations required to develop a similar conductance in the bilayer assay.

The sodium channel voltage sensors behave in a different mode since they are designed for obvious different functions and they, along with other channel fragments, were subjected to extensive biophysical investigations (see e.g. [36–38]). In S4L45s, the presence of proline and its position strongly modulate both voltage-dependence [29] and anti-bacterial activities, but in opposite directions. Of course, the bacterial membrane is negatively charged and the channel-forming properties of S4L45s in neutral or zwitterionic lipid bilayers and in negatively charged ones (POPC/DOPE, 1/1 by mass) were previously compared [28]. To summarize, it turns out that, although the binding of these highly positively charged peptides to negatively charged lipid bilayers was higher than in neutral bilayers [39], transmembrane currents induced by these peptides under the applied voltage were one order smaller in the former lipid mixture than in the latter. Presumably, high electrostatic interactions between the compounds at the membrane interface impeded the voltage-driven membrane insertion of those peptides. On the other hand, channels formed by other highly charged peptides (but not showing the regular pattern of voltage sensors in their sequence) such as cecropin and magainin are (i) not or moderately voltage-dependent and (ii) non-selective within cations (they may even be anion-specific, [11]). Indeed, magainin 1 develops a poorly voltage-dependent macroscopic conductance ($V_e = 20$ mV) and the current intensity starts to be significant for 'physiological' voltages for concentrations around the μM range. Furthermore, the leak is more important than with the peptides studied here and at the single-channel level, currents are large and fail to show the characteristic pattern of fluctuations between different substates. Clearly, its mechanism of action does not obey to the classical and dynamic 'barrel-stave' model. This may apply also to the S4L45s but here, the single-channel conductances are about 10 pS [28] (i.e. 1–2 orders of magnitude smaller than with magainin 1), in agreement with the small pore size derived from the macroscopic conductance.

It is worth keeping in mind that the concentrations used in the anti-bacterial assays were about two orders of magnitude higher than in standard macroscopic experiments. For instance, the MIC for Alm-dUL was around 10^{-5} M (Table 1) whilst the

highest concentration used in current-voltage experiments was in the order of 10^{-7} M (Fig. 6). Still higher concentrations bring the threshold towards a smaller voltage and result in leaky membranes. From the correlations drawn here between MICs and $\langle N \rangle$, it can be inferred that presumably, in the conditions of anti-bacterial assays and despite the different ranges of concentrations mentioned above, there would still be a large excess of monomers freely interacting with the lipids, that is experiencing lateral diffusion as in standard conductance experiments [17,40]. In other words, there would remain a significant fraction of the membrane surface not yet covered by monomers and although they may well form 'rafts' through surface aggregation as in the 'carpet-like' model [41], this large reserve of peptides not yet involved in pore-formation in standard conductance experiments would allow for the building up of a much greater number of barrel-staves in the anti-bacterial assays. Furthermore, it must be postulated that these entities remain discrete pores and do not merge to form a continuous spectrum of 'holes' or defects, as assumed for the highly positively charged magainins of dermaseptins for instance [42,43], eventually leading to a membrane collapse. This presumably no longer applies when much larger hydrophilic sectors preclude the regular barrel-stave arrangement as in other anti-bacterial peptides, e.g. magainins [44], consistent with the poor anti-bacterial activity of magainin 2 on *S. melliferum* [14]. Cooperative interactions of Alm and magainin with lipid bilayers (albeit different from those of the present study) were studied with various techniques including oriented circular dichroism, X-ray lamellar diffraction and neutron in-plane scattering [45–47]. Whereas low concentrations of both agents induced membrane thinning, peptides lying flat within the lipid headgroup region, increased concentrations (pre-determined by the peptide-lipid molar ratio) lead to spontaneous transmembrane insertions allowing pore-forming. The data for Alm are consistent with a pore size compatible with 8–11 monomers according to the lipids used. This is in broad agreement both with molecular modelling [48] and conductance analysis, at a reduced peptide concentration but under applied voltage.

As for the physiological mechanism of peptide toxicity, our observations show that, consistent with previous studies [14,15], the primary effect of Alm on the spiroplasma cell is the rapid abolition of the transmembrane electrical potential (a full collapse being induced within less than 2 min by a 2.5 μM concentration). The consequence is an immediate loss of cell motility followed by a slower cell deformation. This suggests that in spiroplasmas, not only cell motility is coupled to the membrane potential but also the cell shape. Finally, the bactericidal effect of Alm was due to cytolysis, which is a lethal and irreversible phenomenon, since the deformed cells burst into small, DNA-free vesicles. This scenario is consistent with the fact that peptides with a weak channel activity, e.g. the Alm-dUL P14A analog of Alm and the S4L45 peptides, failed to decrease sufficiently the membrane potential for disrupting cell integrity.

Acknowledgements

This work was supported by the Ministère de l'Education nationale de la Recherche et de la Technologie (ACC 'Physico-Chimie des Membranes Biologiques'), the Programme de Recherches Fondamentales en Microbiologie et Maladies Infectieuses et Parasitaires and the Langlois Foundation (Rennes). Thanks are due to Marie-Madeleine Guéguen for technical assistance and Aude Germanangue for processing the manuscript.

References

[1] P. Elsbach, Trends Biotechnol. 8 (1990) 26–30.
[2] A.G. Rao, Mol. Plant-Microbe Interact. 8 (1995) 6–13.
[3] P. Nicolas, A. Mor, Annu. Rev. Microbiol. 49 (1995) 277–304.
[4] I. Cornut, E. Thiaudière and J. Dufourcq, in: R.M. Epand (Ed.), The Amphipathic Helix, CRC Press, Boca Raton, FL, 1993, pp. 173–219.
[5] R.E.W. Hancock, J. Med. Microbiol. 46 (1997) 1–3.
[6] R.E.W. Hancock, R. Lehrer, Trends Biotechnol. 16 (1998) 82–88.
[7] B. Bechinger, J. Membr. Biol. 156 (1997) 197–211.
[8] A. Colotto, D.P. Kharakoz, K. Lohner, P. Laggner, Biophys. J. 65 (1993) 2360–2367.
[9] H. Duclohier, G. Molle, F. Spach, Biophys. J. 56 (1989) 1017–1021.

[10] S.J. Ludtke, K. He, W.T. Heller, T.A. Harroun, L. Yang, H.W. Huey, Biochemistry 35 (1996) 13723–13728.
[11] H. Duclohier, Toxicology 87 (1994) 175–188.
[12] W.C. Jen, G.A. Jones, D. Brewer, V.O. Parkinson, A. Taylor, J. Appl. Bacteriol. 63 (1987) 293–298.
[13] J.W. Payne, R. Jakes, B.S. Hartley, Biochem. J. 117 (1970) 757–766.
[14] L. Béven, H. Wróblewski, Res. Microbiol. 148 (1997) 163–175.
[15] L. Béven, D. Duval, S. Rebuffat, F.G. Riddell, B. Bodo, H. Wróblewski, Biochim. Biophys. Acta 1372 (1998) 78–90.
[16] M. Dathe, C. Kaduk, E. Tachikawa, M.F. Melzig, H. Wenschuch, M. Bienert, Biochim. Biophys. Acta 1370 (1998) 175–183.
[17] D.S. Cafiso, Annu. Rev. Biophys. Biomol. Struct. 23 (1994) 141–165.
[18] G.A. Woolley, B.A. Wallace, J. Membr. Biol. 129 (1992) 109–136.
[19] R.O. Fox, F.M. Richards, Nature 300 (1982) 325–330.
[20] J.E. Hall, I. Vodyanoy, T.M. Balasubramanian, G.R. Marshall, Biophys. J. 45 (1984) 233–247.
[21] G.N. Filatov, T.P. Nguyen, S.D. Kraner, R.L. Barchi, J. Gen. Physiol. 111 (1998) 703–715.
[22] T.B. Clark, R.F. Whitcomb, J.G. Tully, C. Mouchès, C. Saillard, J.-M. Bové, H. Wróblewski, P. Carle, D.L. Rose, R.B. Henegar, D.L. Williamson, Int. J. Syst. Bacteriol. 35 (1985) 296–308.
[23] S. Razin, D. Yogev, Y. Naot, Microbiol. Mol. Biol. Rev. 62 (1992) 1094–1156.
[24] Å. Wieslander, M.J. Boyer and H. Wróblewski, in: J. Maniloff, R.N. McElhaney, L.R. Finch and J.B. Baseman (Eds.), Mycoplasmas: Molecular Biology and Pathogenesis, ASM Press, Washington, DC, 1992, pp. 93–112.
[25] L. Béven, L. Chaloin, P. Vidal, F. Heitz, H. Wróblewski, Biochim. Biophys. Acta 1329 (1997) 357–369.
[26] Y. Fleury, V. Vouille, L. Béven, M. Amiche, H. Wróblewski, A. Delfour, P. Nicolas, Biochim. Biophys. Acta 1396 (1998) 228–236.
[27] H. Wróblewski, D. Robic, D. Thomas, A. Blanchard, Ann. Microbiol. (Inst. Pasteur, Paris) 135A (1984) 73–82.
[28] M. Brullemans, O. Helluin, J.-Y. Dugast, G. Molle, H. Duclohier, Eur. Biophys. J. 23 (1994) 39–49.
[29] O. Helluin, S. Bendahhou, H. Duclohier, Eur. Biophys. J. 27 (1998) 595–604.
[30] G. Molle, J.-Y. Dugast, H. Duclohier, G. Spach, Biochim. Biophys. Acta 938 (1988) 310–314.
[31] G. Molle, J.-Y. Dugast, G. Spach, H. Duclohier, Biophys. J. 70 (1996) 1669–1675.
[32] W.C. Russell, C. Newman, D.H. Williamson, Nature 253 (1975) 461–462.
[33] H. Duclohier, H. Molle, J.-Y. Dugast, G. Spach, Biophys. J. 63 (1992) 868–873.
[34] T. Iwata, S. Lee, O. Oishi, H. Aoyagi, M. Ohno, K. Anzai, Y. Kirino, G. Sugihara, J. Biol. Chem. 269 (1994) 4928–4933.
[35] J. Breed, I.D. Kerr, G. Molle, H. Duclohier, M.S.P. Sansom, Biochim. Biophys. Acta 1330 (1997) 103–109.
[36] S.J. Opella, J. Gesell, A.P. Valente, F.M. Marassi, M. Oblatt-Montal, W. Sun, A. FerrerMonteil, M. Montal, Chemtracts-Biochem. Mol. Biol. 10 (1997) 153–174.
[37] H. Duclohier, O. Helluin, P. Cosette, A.R. Schoofs, S. Bendahhou, H. Wróblewski, Chemtracts-Biochem. Mol. Biol. 10 (1997) 189–206.
[38] Y. Shai, Chemtracts-Biochem. Mol. Biol. 10 (1997) 207–224.
[39] D. Rapaport, M. Danin, E. Gazit, Y. Shai, Biochemistry 31 (1992) 8868–8875.
[40] O. Helluin, J.Y. Dugast, G. Molle, A.R. Mackie, S. Ladha, H. Duclohier, Biochim. Biophys. Acta 1330 (1997) 234–292.
[41] Y. Shai, Trends Biochem. Sci. 20 (1995) 460–464.
[42] L. Jacob and M. Zasloff, in: H.G. Boman, J. Marsh and J.A. Goode (Eds.), Antimicrobial Peptides, John Wiley and Sons, New York, Ciba Found. Symp. 186, 1994, pp. 197–216.
[43] P. La Rocca, Y. Shai, M.S.P. Sansom, Biophys. Chem. 76 (1999) 145–159.
[44] T. Wieprecht, M. Dathe, M. Beyermann, E. Krause, W.L. Maloy, D.L. MacDonald, M. Bienert, Biochemistry 36 (1997) 6124–6132.
[45] S.J. Ludtke, K. He, Y. Wu, H.W. Huang, Biochim. Biophys. Acta 1990 (1994) 181–184.
[46] Y. Wu, K. He, S.J. Ludtke, H.W. Huang, Biophys. J. 68 (1995) 2361–2369.
[47] K. He, S.J. Ludtke, H.W. Huang, D.L. Worcester, Biochemistry 34 (1995) 15614–15618.
[48] J. Breed, R. Sankararamakrishnan, I.D. Kerr, M.S.P. Sansom, Biophys. J. 70 (1996) 1643–1661.